# Residence time of buoyant objects in drowning machines

Gustavo Gioia[a], Pinaki Chakraborty[b,1], Stefan F. Gary[a,2], Carlo Zuñiga Zamalloa[a], and Richard D. Keane[a]

[a]Department of Mechanical Science and Engineering, University of Illinois, Urbana, IL 61801; and [b]Department of Geology, University of Illinois, Urbana, IL 61801

Edited* by Susan W. Kieffer, University of Illinois, Urbana, IL, and approved February 15, 2011 (received for review October 10, 2010)

**Hydraulic jumps are a common feature of rivers and waterways, where they can be found close to spillways, weirs, rocky ledges, and boulders. People adrift upstream of a hydraulic jump are liable to become trapped in the turbulent roller of the hydraulic jump. For this reason, hydraulic jumps have been termed "drowning machines" and are recognized as a public hazard. We use experiments and theory to show that on average a buoyant object spends a time $\tau/p$ trapped in a jump, where $\tau$ is the period of a harmonic process inherent in the jump, and $p$ is the probability that the object will escape in any time interval $\tau$. The probability $p$ is governed by the statistical theory of extreme values and depends primarily on the ratio between the density of the object and the density of the fluid. We use our results to draw conclusions that might prove to be useful to public-safety agencies intent on carrying out tests in drowning machines. Our results can also be used to predict the amount of flotsam that accumulates at the toe of a hydraulic jump.**

dimensional analysis | extremal statistics | turbulence

A hydraulic jump forms in an open stream where a fast and shallow, supercritical flow transitions downstream to a comparatively slower and deeper, subcritical flow (1) (Fig. 1 *A* and *B*). The hydraulic jump consists of a turbulent roller in which the kinetic energy of the supercritical flow is dissipated in order to match the kinetic energy of the subcritical flow (1). Thus hydraulic jumps are often engineered to prevent erosion downstream of dams, weirs, spillways, and canoe chutes (2). Hydraulic jumps also occur spontaneously in river rapids (3), where large hydraulic jumps may form upstream of rocky ledges and boulders (4). Plants, trash, logs, boats, and sometimes even animals and people may pass through a hydraulic jump. To pass through a jump, a buoyant object must dip into the flow and move under the roller to emerge on the surface of the subcritical flow downstream of the roller (trajectory A, Fig. 1*C*). Before the object finds its way there, it spends some time trapped in the jump. As demonstrated by the type of sign found in proximity of drowning machines (Fig. 1*D*), the outcome is often fatal. For example, in 1983 a raft was overturned and its occupants became trapped in a 6-m-high jump on the Colorado River. One person drowned and dozens were seriously injured (4). Our goal is to relate the statistical properties of the time that a buoyant object spends in a jump to the attributes of the jump and the buoyant object.

We carry out experiments in an open channel of uniform rectangular cross-section. The fluid is tap water. To create a hydraulic jump, we start with a supercritical flow, that is, a flow of Froude number $\mathrm{Fr} > 1$ (caption of Fig. 1*B*). This supercritical flow spans the length of the channel, from inlet to outlet. We then place a step at the outlet; the water builds up there, and after some time a jump becomes established at about the midpoint between the inlet and the outlet (Fig. 1 *A* and *B*). Upstream of the jump, the flow is the same as before; downstream of the jump, the flow is subcritical, and the Froude number $\mathrm{Fr}' < 1$ (caption of Fig. 1*B*).

We drop a buoyant spherical ball in the flow upstream of the jump and measure the time the ball spends in the jump before making it to the surface of the flow downstream of the jump. We call this time the *residence time*. The residence time can vary widely from trial to trial. After measuring many residence times, we compute the cumulative probability distribution $Q(t)$, that is, the probability that the ball will remain in the jump after an elapsed time $t$. Plots of several cumulative probability distributions are shown in Fig. 2. (See *SI Appendix* for further details.)

To help interpret the plots of Fig. 2, we describe the behavior of a ball in a hydraulic jump. When the ball reaches the toe of the jump, it lingers there for a while before it dips into the flow. Where the residence time is brief, the ball dips and is promptly advected under the roller (trajectory A, Fig. 1*C*). The ball has escaped.

Where the residence time is longer, the ball may undergo numerous cycles before it escapes. In each cycle the ball dips, is caught into the roller, and returns to its original position at the toe of the jump (trajectory B, Fig. 1*C*). Eventually, the ball dips and is advected downstream without getting caught into the roller.

To each of the cycles of the previous paragraph we ascribe the same characteristic time $\tau$ and the same probability of escape, $p$. The probability that a ball will remain in a jump after $n$ cycles is $(1-p)^n$, and the residence time of a ball that escapes after $n$ cycles is $t = n\tau + t_0$, where $t_0$ is the time needed for the ball to move under the roller (trajectory A, Fig. 1*C*). The cumulative probability distribution can be expressed in the form $Q(t) = (1-p)^{(t-t_0)/\tau}$ or $\ln Q(t) = st + q$, where $s \equiv \ln(1-p)/\tau$ and $q \equiv -t_0 \ln(1-p)/\tau$. For any combination of jump and ball the values of $s$ and $q$ can be extracted directly from a plot of $\ln Q(t)$ (Fig. 2) and used to compute $p$ and $t_0$,

$$p = 1 - \exp s\tau, \qquad [1]$$

and $t_0 = -q/s$. We refer to $s$ as the "slope of the cumulative probability distribution $Q(t)$."

Consider the characteristic time $\tau$. We argue that $\tau$ is the period of a harmonic process inherent in the jump (5–8). Thus $\tau$ may depend on the five variables of the jump—$V$ (or $V'$), $h$ (or $h'$), $g$, $\rho$, and $\mu$, where $\rho$ and $\mu$ are the density and the viscosity of the fluid, respectively. From Buckingham's $\Pi$ theorem of dimensional analysis (9), the functional relation between $\tau$ and the five variables of the jump can be expressed in the form of an equivalent functional relation among three dimensionless variables. We choose the dimensionless variables $\tau g/V'$, $\mathrm{Fr} \equiv V/\sqrt{gh}$, and $\mathrm{Re} \equiv \rho V h/\mu$ (the Reynolds number of the jump, which quantifies the relative importance of the inertial forces and the viscous

Author contributions: G.G., P.C., and R.D.K. designed research; G.G., P.C., S.F.G., C.Z.Z., and R.D.K. performed research; G.G., P.C., and S.F.G. analyzed data; G.G. wrote the manuscript; and S.F.G, P.C., and G.G. wrote the SI Appendix.

The authors declare no conflict of interest.

*This Direct Submission article had a prearranged editor.

[1]To whom correspondence should be addressed. E-mail: chakrabo@uiuc.edu.

[2]Present address: Division of Earth and Ocean Sciences, Duke University, Durham, NC 27708.

This article contains supporting information online at www.pnas.org/lookup/suppl/doi:10.1073/pnas.1015183108/-/DCSupplemental.

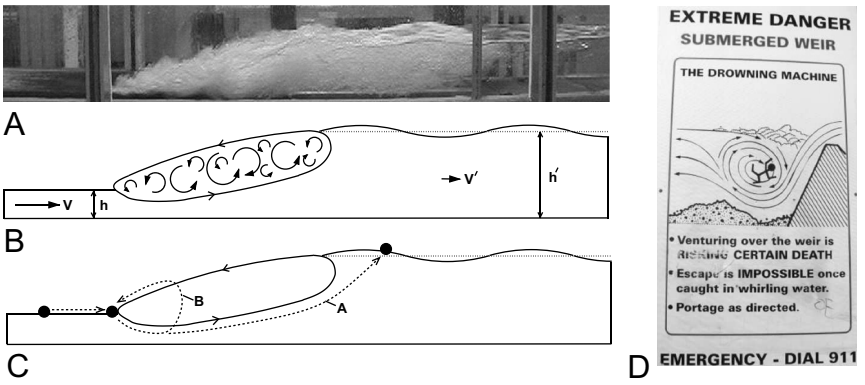


**Fig. 1.** Hydraulic jumps. (*A*) Side view of a hydraulic jump in the laboratory. The flow is from left to right. (*B*) Side view of a hydraulic jump (schematic). The curly arrows represent the turbulent eddies (or fluctuations) of the roller. $V$ and $h$ are, respectively, the average velocity and the average depth of the supercritical flow; $V'$ and $h'$ are, respectively, the average velocity and the average depth of the subcritical flow. In the supercritical flow the inertial forces dominate over the gravitational forces, so that the Froude number $\mathrm{Fr} \equiv V/\sqrt{gh} > 1$ (1), where $g$ is the gravitational acceleration. In the subcritical flow the gravitational forces dominate over the inertial forces, so that the Froude number $\mathrm{Fr}' \equiv V'/\sqrt{gh'} < 1$ (1). For any given jump, $V$, $h$, $V'$, and $h'$ are related by the equations of conservation of momentum and mass, which may be written as $h' = h(\sqrt{1+8\mathrm{Fr}^2}-1)/2$ and $V' = Vh/h'$ (1). It follows that $\mathrm{Fr}' = \mathrm{Fr}[(\sqrt{1+8\mathrm{Fr}^2}-1)/2]^{-3/2}$. (*C*) A buoyant object escapes the jump (trajectory A) and is caught into the roller (trajectory B). (*D*) Drowning machines (19) have proven to be so troublesome in highly populated areas that municipalities are having recourse to extreme measures. For example, the city of Calgary, AB, Canada, is currently undertaking a $6.4 million project to eliminate a drowning machine on the Bow River. The picture was taken in August 2010, amid the construction work. Note that the drowning machine sketched in the picture is a "submerged hydraulic jump," a special case of a hydraulic jump. We have carried out experiments only on exposed hydraulic jumps, but in *SI Appendix* we discuss how to adapt our analysis to the case of submerged hydraulic jumps.

forces in the jump). For most jumps $\mathrm{Re} \gg 1$ (in each of our experiments $\mathrm{Re} > 7.5 \times 10^4$), and the viscous forces are negligible as compared to the inertial forces. We can therefore assume that $\tau g/V'$ depends only on Fr.

To relate $\tau g/V'$ to Fr, we identify $\tau$ with the period of a wave that forms on the surface of the flow downstream of a jump (Fig. 1 *A* and *B*). By measuring the period of that wave for several jumps, we compute data points $(\tau g/V', \mathrm{Fr})$. Based on a plot of these data points (Fig. 3), we write the semiempirical formula $\tau = 3.2(\mathrm{Fr}-1)V'/g$.

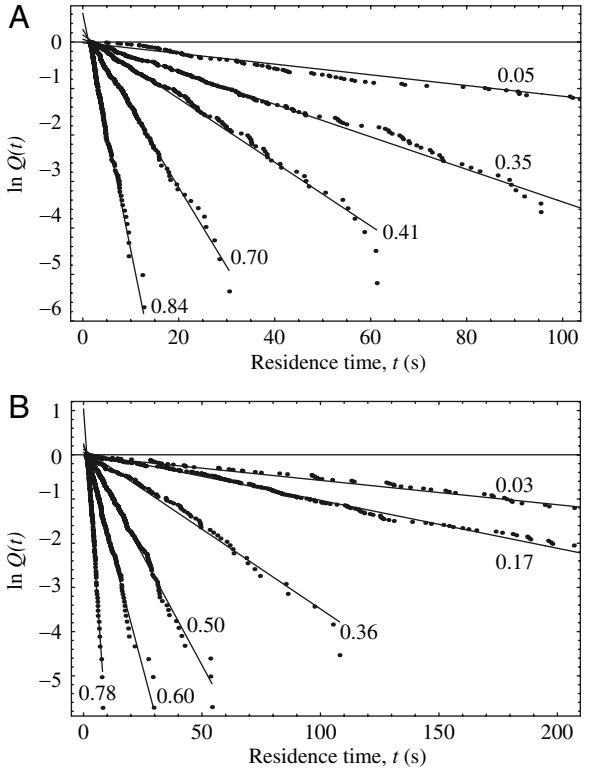


**Fig. 2.** Cumulative probability distributions $Q(t)$ of the residence time $t$. Each distribution is a straight line—the best fit to a set of data points for a given combination of jump and ball. A set of data points consists of data points $[t_m, \ln(m/M)]$, $m = 1$ to $M$, where $M$ is the number of measurements of the residence time and $t_1, t_2, \ldots, t_M$ are the residence times ordered longest to shortest. Next to each distribution, we indicate the ball density (in g/cm$^3$). The Froude number is about (*A*) 4 and (*B*) 5.

Consider next the probability $p$ that the ball will not be caught into the roller in a given cycle (trajectory A, Fig. 1*C*). As the ball is advected under the roller, it may be kept bouncing off the keel of the roller by a series of collisions with the turbulent eddies (or fluctuations) of the roller. The turbulent eddy of collision $i$ has a revolving velocity $v_i$, and $x$ is the smallest value of $v_i$, $x \equiv \min(v_1, v_2, \cdots, v_N)$, where $N$ is the number of collisions. We propose that the ball will not be caught into the roller if $x \geq x_c$, where $x_c$ is a threshold value. If $N \to \infty$ and the $v_i$s are sampled from a common distribution (10–13) in the domain of attraction (14) of the extreme-value distribution of type I (15), then the probability that $x \geq x_c$ will be

$$p = 1 - \exp(-\exp X_c). \qquad [2]$$

Here $X_c \equiv (x_c - \alpha)/\beta$, $\beta\pi/\sqrt{6}$ is the standard deviation of $x$, $\alpha - \Gamma\beta$ is the mean value of $x$, and $\Gamma$ is the Euler–Mascheroni constant. Now, the variable $X_c$ may depend on the five variables of the jump ($V$, $h$, $g$, $\rho$, and $\mu$) and the two variables of the ball (the

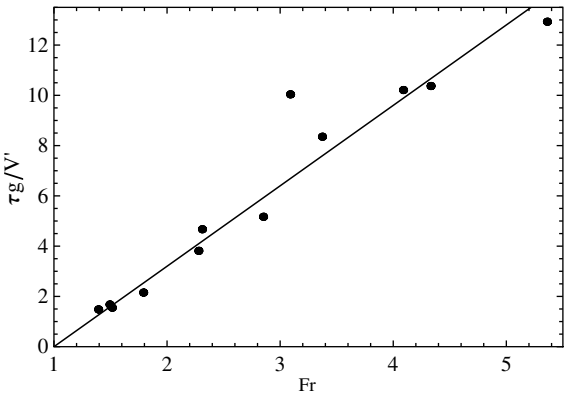


**Fig. 3.** Experimental data on the characteristic time $\tau$. The data points are from measurements of the period of the wave found on the surface of the flow downstream of a jump. The straight line corresponds to $\tau g/V' = 3.2(\mathrm{Fr}-1)$.

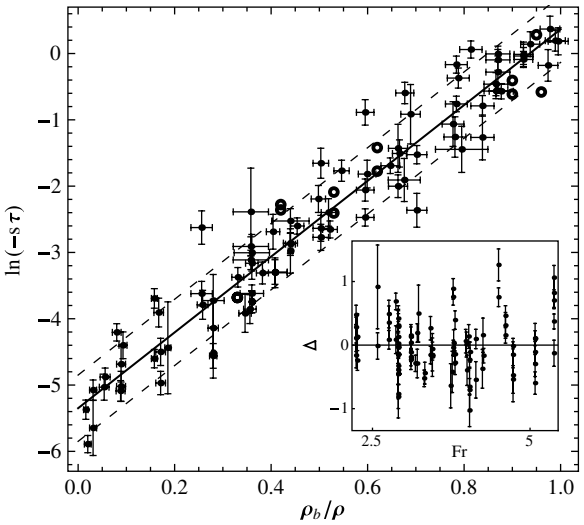


**Fig. 4.** Experimental data points $[\ln(-s\tau),\rho_b/\rho]$. The filled circles with error bars are the data points for spherical balls. (See *SI Appendix* for a description of the method used to calculate the error bars.) The solid line is the optimal fit of Eq. **4** to these data points, and the dashed lines are the optimal fit $\pm \ln 2$. The open circles are the data points for a bottle and a pillbox (see *SI Appendix* for further details). (*Inset*) Plot of the vertical scatter $\Delta$ (the signed vertical distance between the optimal fit and each data point) as a function of Fr. We discern no clear correlation between $\Delta$ and Fr.

diameter $d$ and the density $\rho_b$). (See *SI Appendix* for further details.) We apply Buckingham's $\Pi$ theorem once again and choose the dimensionless variables $X_c$, $\rho_b/\rho$, Fr, Re, and $\mathrm{Re}_b \equiv \rho V d/\mu$ (the Reynolds number of the ball). For most jumps $\mathrm{Re} \gg 1$ (as we argued before), and for most combinations of jump and ball $\mathrm{Re}_b \gg 1$ (in each of our experiments $\mathrm{Re}_b > 5 \times 10^4$, consistent with our assumption that the interactions between the ball and the eddies of the roller are collisional). Thus we can assume that $X_c$ is independent of both Re and $\mathrm{Re}_b$. Further, we assume that $X_c$ is largely independent of Fr (we will come back to this assumption later on) and therefore that $X_c$ depends only on $\rho_b/\rho$. As $0 < \rho_b/\rho < 1$, we use the estimate

$$X_c = a + b\rho_b/\rho, \qquad [3]$$

where $a$ and $b$ are dimensionless constants. This estimate corresponds to the first two terms of the Taylor expansion of $X_c$ about $\rho_b/\rho = 0$.

By combining Eqs. **1**–**3**, we conclude that

$$\ln(-s\tau) = a + b\rho_b/\rho, \qquad [4]$$

where $s$ is the slope of the cumulative probability distribution $Q(t)$ and $\tau = 3.2(\mathrm{Fr} - 1)V'/g$. To test Eq. **4**, we compute a data point $[\ln(-s\tau),\rho_b/\rho]$ for each combination of jump and ball in our experiments and plot all 87 data points as shown in Fig. 4. By fitting Eq. **4** to the data points, we determine the optimal values $a = -5.35$ and $b = 5.72$. Using these optimal values, we estimate the probability that a denseless ball will escape the jump in any given cycle, $p = p_0 \equiv 1 - \exp(-\exp a) = 0.0047$, and the probability that a ball of the same density as the fluid will escape the jump in any given cycle, $p = p_1 \equiv 1 - \exp[-\exp(a + b)] = 0.76$.

The scatter in Fig. 4 exceeds the error bars of many data points. From Fig. 4, *Inset*, we conclude that the scatter does not hide a systematic dependence on Fr (recall our assumption that $X_c$ is independent of Fr). But Eq. **2** holds only asymptotically, for $N \to \infty$; convergence is known to be slow (14); and the excess scatter may be ascribed to an insufficient number of collisions per cycle.

So far we have carried out experiments with spherical balls. To show that the theory can be applied more widely, we carry out several additional experiments with a bottle and a pillbox partially filled with water. The corresponding data points, shown as open circles in Fig. 4, are indistinguishable from the data points that we obtained earlier.

To summarize, the average residence time of a buoyant object in a hydraulic jump can be estimated as $\tau/\{1 - \exp[-\exp(-5.35 + 5.72\rho_b/\rho)]\}$, where $\tau$ is a characteristic period of the jump, $\rho_b$ is the density of the object, and $\rho$ is the density of the fluid. In a typical drowning machine the residence time can vary from a few minutes for a very light object ($\rho_b/\rho \approx 0$) to about 1 s for an object that is barely buoyant ($\rho_b/\rho \approx 1$). Note, however, that an increase in $\rho_b/\rho$ leads to a sizable lessening in residence time only at relatively large values of $\rho_b/\rho$. Thus the average residence time of a person should not exceed a few seconds, regardless of whether a life jacket is worn ($\rho_b/\rho \approx 0.85$) or not worn ($\rho_b/\rho \approx 0.95$), provided that the person remains passive (as the buoyant objects of our experiments) (16–18). But far from remaining passive, people will typically swim frantically to stay away from the downward pull upstream of the jump, which is precisely where a chance may be had of escaping by being advected under the roller. Public-safety agencies might wish to carry out tests in which participants are instructed either to remain passive, perhaps curled in the fetal position, or to direct any expenditure of energy toward gaining depth under water. The notion that a life jacket can significantly delay escape from a drowning machine cannot be reconciled with our results.

**ACKNOWLEDGMENTS.** Michael C. Dameron, John C. Griffith, Je I. Ryu, William F. Burgoyne, Federico Scholcoff, and especially Paulo Zandonade provided much help with the experiments. We thank James W. Phillips (University of Illinois, Urbana, IL) for the photograph of Fig. 1*A*. We thank Zhongchao Tan (University of Waterloo, ON, Canada) for the photograph of Fig. 1*D*. This work was financed in part by National Science Foundation Division of Materials Research Grant 10-44901. P.C. acknowledges support from The Roscoe G. Jackson II Research Fellowship.

1. Chow VT (1988) *Open-Channel Hydraulics* (McGraw-Hill, New York).
2. Chanson H (1999) *The Hydraulics of Open Channel Flow* (Wiley, New York).
3. Leopold LB, Wolman MG, Miller JP (1995) *Fluvial Processes in Geomorphology* (Dover, Mineola, NY).
4. Kieffer S (1985) The 1983 hydraulic jump in Crystal Rapid: Implications for river-running and geomorphic evolution in the Grand Canyon. *J Geol* 93:385–406.
5. Long D, Rajaratnam N, Steffler P, Smy P (1991) Structure of flow in hydraulic jumps. *J Hydraul Res* 29:207–218.
6. Mossa M (1999) On the oscillating characteristics of hydraulic jumps. *J Hydraul Res* 37:541–558.
7. Mossa M, Tolve U (1998) Flow visualization in bubbly two-phase hydraulic jump. *J Fluid Eng-T ASME* 120:160–165.
8. Hoyt J, Sellin R (1989) Hydraulic jump as mixing layer. *J Hydraul Eng-ASCE* 115:1607–1614.
9. Barenblatt GI (1986) *Scaling, Self-Similarity, and Intermediate Asymptotics* (Cambridge Univ Press, Cambridge, UK).
10. Chanson H (2007) Bubbly flow structure in hydraulic jump. *Eur J Mech B-Fluid* 26:367–384.
11. Tavoularis S, Corrsin S (1981) Experiments in nearly homogenous turbulent shear flow with a uniform mean temperature gradient. Part 1. *J Fluid Mech* 104:311–347.
12. Dinavahi S, Breuer K, Sirovich L (1995) Universality of probability density functions in turbulent channel flow. *Phys Fluids* 7:1122–1129.
13. Tsuji Y, Nakamura I (1999) Probability density function in the log-law region of low Reynolds number turbulent boundary layer. *Phys Fluids* 11:647–658.
14. Castillo E, Hadi AS, Balakrishnan N, Sarabia JM (2005) *Extreme Value and Related Models with Applications in Engineering and Science* (Wiley, Hoboken, NJ).
15. Weisstein EW Gumbel Distribution. (MathWorld—a Wolfram Web resource), http://mathworld.wolfram.com/GumbelDistribution.html.
16. Herman I (2007) *Physics of the Human Body* (Springer, Berlin).
17. Macintosh RR, Pask EA (1957) The testing of life-jackets. *Brit J Ind Med* 14:168–176.
18. Personal Flotation Device Manufacturers Association, Facts about life jackets (http://www.pfdma.org/local/downloads/documents/pfdmabrochure.pdf).
19. Leutheusser H, Birk W (1991) Drownproofing of low overflow structures. *J Hydraul Eng-ASCE* 117:205–213.